

# Atomistic Study of the Thermal Stress due to Twin Boundaries

Dengke Chen

Department of Mechanical Engineering,  
University of Houston,  
Houston, TX 77204

Yashashree Kulkarni<sup>1</sup>

Department of Mechanical Engineering,  
University of Houston,  
Houston, TX 77204  
e-mail: ykulkarni@uh.edu

*There is compelling evidence for the critical role of twin boundaries in imparting the extraordinary combination of strength and ductility to nanotwinned metals. This paper presents a study of the thermal expansion of coherent twin boundaries (CTBs) at finite temperature by way of atomistic simulations. The simulations reveal that for all twin boundary spacings  $d$ , the thermal expansion induced stress varies as  $1/d$ . This surprisingly long-range effect is attributed to the inhomogeneity in the thermal expansion coefficient due to the interfacial regions. [DOI: 10.1115/1.4029405]*

*Keywords: coherent twin boundaries, molecular dynamics, thermal expansion coefficient, thermal stress*

## 1 Introduction

Research over the past decade has provided compelling evidence that a novel class of materials known as nanotwinned metals may be the optimal motifs for the design of high-strength high-ductility materials [1–3]. Nanotwinned fcc metals are designed by the introduction of CTBs within ultrafine crystalline metals having a grain size of a few hundred nanometers. The typical twin lamella thickness within each grain ranges between 20 and 100 nm. The numerous studies performed till date reveal that the CTBs have a very high shear strength compared to most grain boundaries (GBs) and are also effective barriers to dislocation motion. This leads to a Hall–Petch type strengthening mechanism associated with GBs [4–6]. However, a unique feature of the CTBs is that the twin planes are also slip planes for fcc metals which enables them to accommodate large plastic strains by absorption of dislocations thus enhancing ductility [7]. In addition, experimental studies have revealed more promising characteristics such as good creep response, thermal stability, and radiation response [8–10]. Very recent studies have made it possible to fabricate nanotwinned nanowires with twin spacing on the order of a mere few angstroms which demonstrate extraordinary strength [11–13]. The smallest twin lamella in these specimens has only two atomic layers separating adjacent twin boundaries. While these superior nanostructures certainly open up exciting avenues for the applications of nanotwinned materials, they also call for a closer examination of the stability of these structural motifs especially at finite temperature. In this paper, we perform atomistic simulations at high temperatures to compute the thermal stress due to the presence of twin boundaries as a function of the twin boundary spacing and explain our results by means of a simple thermal expansion based analysis.

## 2 Simulation Method

Molecular dynamics simulations were performed on Cu based on the embedded-atom-method interatomic potential developed by Mishin et al. [14] using LAMMPS [15]. As shown in Fig. 1, the nanotwinned specimens were oriented along the  $[\bar{1}12]$ ,  $[\bar{1}1\bar{1}]$ , and  $[\bar{1}\bar{1}0]$  crystallographic directions. Thus, the  $Y$ -direction was aligned normal to the plane of the twin boundaries. The simulation cell dimensions in the lateral ( $X$  and  $Z$ ) directions were  $L_x \approx 70 \text{ \AA}$ , and  $L_z \approx 70 \text{ \AA}$ , with periodic boundary conditions applied in both

directions. Simulations were performed for three different specimen heights, specifically, 124  $\text{\AA}$ , 248  $\text{\AA}$ , and 372  $\text{\AA}$ , to take into account any dependence of the stress calculations on the length in the normal direction. The CTB spacing was varied from 0.6 nm to 6 nm. Since the CTB spacing was kept uniform within a specimen, each specimen with constant height but different CTB spacing contained different number of CTBs.

The simulation cell was first relaxed at zero temperature using energy minimization. Keeping the atoms on the upper and lower boundaries fixed, the structure was equilibrated at 800 K by running molecular dynamics for 100 ps using the Nose-Hoover thermostat such that the stresses in the lateral directions were completely relaxed to zero. The virial stress formulation was used for estimating the average stress. We note that there is thermal stress in the  $Y$ -direction since it is not allowed to relax due to the fixed displacement boundary conditions at the top and bottom surfaces. In order to isolate the contribution of the CTBs to the calculated stress, we need to subtract the contribution of the thermal stress resulting in a single crystal. To this end, a corresponding single crystal specimen with identical dimensions, orientation, and boundary conditions was created and equilibrated as above. We thereby obtain the contribution of the twin boundaries to the thermal stress as

$$\sigma = \sigma_{\text{NT}} - \sigma_{\text{SC}} \quad (1)$$

where  $\sigma_{\text{NT}}$  denotes the normal stress in the  $Y$ -direction calculated for the nanotwinned specimen and  $\sigma_{\text{SC}}$  denotes the normal stress in the  $Y$ -direction calculated for the corresponding single crystal specimen without CTBs. To assess the effect of the simulation cell size on the stress calculations, we also performed the simulation on a larger specimen with dimensions  $210 \text{ \AA} \times 250 \text{ \AA} \times 240 \text{ \AA}$ . The results changed only negligibly.

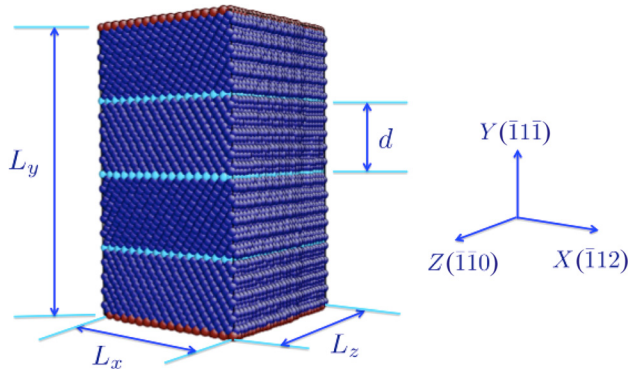
## 3 Simulation Results

Figure 2 shows the variation of the stress  $\sigma$  as a function of  $1/d$ , for specimen with different height  $H$  at 800 K. The relationship is linear and indicates that an increase in the CTB separation leads to a decrease in the thermal stress. For the different heights considered in our simulations, we also observe that for a fixed CTB spacing, the thermal stress  $\sigma$  is independent of the height of the specimen, and hence the number of CTBs.

We now consider simulations in which the number of CTBs,  $N$ , is held constant while the CTB spacing,  $d$ , is varied. For the sake of illustration, Fig. 3 shows the atomistic structure of a typical specimen with three CTBs ( $N = 3$ ) and different  $d$ . In these cases,  $d$  is the CTB spacing and is also equal to the distance between the

<sup>1</sup>Corresponding author.

Contributed by the Applied Mechanics Division of ASME for publication in the JOURNAL OF APPLIED MECHANICS. Manuscript received November 11, 2014; final manuscript received December 16, 2014; accepted manuscript posted December 18, 2014; published online January 7, 2015. Assoc. Editor: Chad M. Landis.



**Fig. 1** Atomistic structure of a nanotwinned specimen showing the crystallographic orientation. The specimen contains three equally spaced CTBs separated by distance  $d$ .

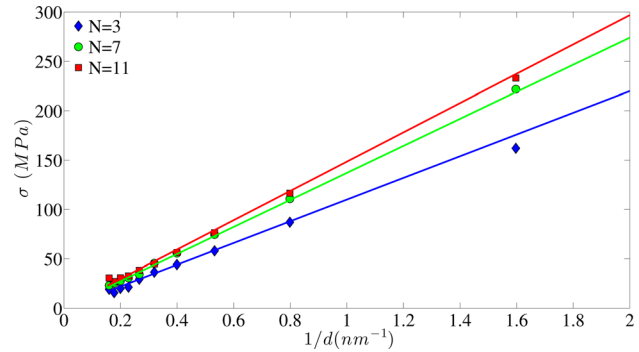


**Fig. 4** Variation of the stress  $\sigma$  with CTB density,  $1/d$ , for specimens with different number of CTBs,  $N$ , at 800 K. All cases show a linear dependence.

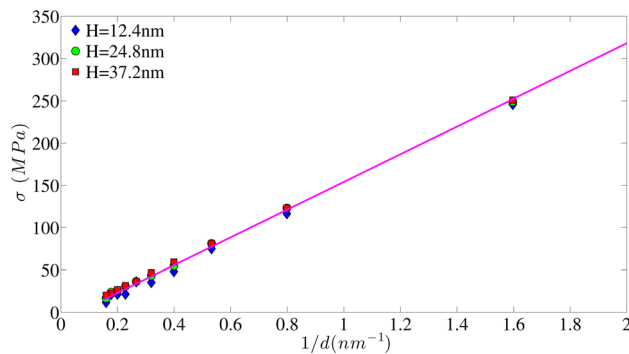


**Fig. 2** Variation of the stress  $\sigma$  with CTB density  $1/d$ , for specimens with different height ( $H$ ) at 800 K. All cases show a linear relation.

last CTBs and the adjoining top or bottom surfaces. Following the simulation procedure described above, we obtain the relationship between the thermal stress  $\sigma$  and the CTB spacing  $d$ . The results for specimens with different number of CTBs are compiled in Fig. 4. All the cases exhibit a  $1/d$  dependence of the thermal stress due to twin boundaries at finite temperature. We also note that as  $N$  decreases, there is a decrease in the slope of the curves. This is possibly a result of size effects in specimens with very few atomic

layers, and will be discussed again in Sec. 5. Nevertheless, taking together the simulation results shown in Figs. 2 and 4, we observe that the linear dependence of the thermal stress on  $1/d$  is rather insensitive to the number of CTBs or sample dimensions.

#### 4 Analysis

Here, we investigate the role of the thermal expansion to explain the  $1/d$  dependence of the thermal stress observed in simulations. Past research has shown that the thermal expansion coefficient of nanostructured metals is indeed different from their single crystal counterparts and is strongly grain-size dependent [16–20]. This is due to the change in the coefficient of thermal expansion in the proximity of the GBs owing to the mismatch in orientation. Following the work of Phillpot [16], we consider a periodic or infinitely long nanotwinned structure as comprising of two parts: the interfacial region around the CTB and the bulk region that is single crystalline (Fig. 5). We assume that each of these regions has a distinct thermal expansion coefficient denoted by  $\alpha_{\text{TB}}$ , and  $\alpha_{\text{SC}}$ , respectively. It is reasonable to assume that  $\alpha_{\text{TB}}$  and  $\alpha_{\text{SC}}$  are material properties which means that they are independent of the CTB spacing  $d$ . Since the stress in the  $Y$ -direction (normal to the CTBs) is uniform, the effective thermal expansion coefficient  $\alpha_{\text{NT}}$  for the nanotwinned structure can be calculated by adding the thermal expansion from the CTB region and the bulk region. Thus, we have

$$2d\alpha_{\text{NT}} = 2\Lambda\alpha_{\text{TB}} + (2d - 2\Lambda)\alpha_{\text{SC}} \quad (2)$$

where  $\Lambda$  is the thickness of the interfacial region. This can be reduced to

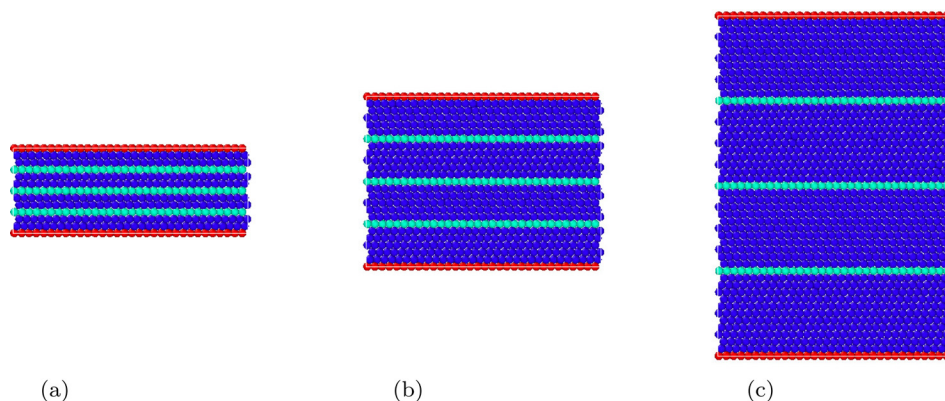


**Fig. 3** Atomistic structure of a typical specimen containing three equally spaced CTBs ( $N=3$ ) with different spacings  $d$ , and hence different specimen heights.

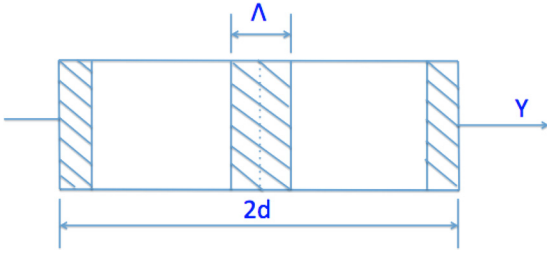


**Fig. 5 Schematic of a CTB superlattice of  $2d$  length. There is an interface region (hatched area) of width  $\Lambda$  around each TB (shown by the dotted line in the middle). The hatched area on either ends is of width  $\Lambda/2$  due to periodicity. The rest of the region is considered a perfect crystal.**

$$\alpha_{NT} - \alpha_{SC} = \Lambda(\alpha_{TB} - \alpha_{SC}) \frac{1}{d} \quad (3)$$

This is the difference between the thermal expansion coefficient of the nanotwinned structure and the single crystal structure. Assuming linear thermal expansion, linear elasticity yields the thermal stress as  $\sigma = \alpha E \Delta T$ , where  $E$  is the Young's modulus. Thus, Eq. (1) can be simplified as

$$\begin{aligned} \sigma &= \sigma_{NT} - \sigma_{SC} \\ &= \alpha_{NT} \Delta T E_{NT} - \alpha_{SC} \Delta T E_{SC} \\ &\approx \Lambda E_{SC} \Delta T (\alpha_{TB} - \alpha_{SC}) \frac{1}{d} \propto \frac{1}{d} \end{aligned} \quad (4)$$

which shows a linear dependence of the thermal stress on  $1/d$ , consistent with the atomistic simulations presented earlier. In the above derivation, it was assumed that  $E_{NT} \approx E_{SC}$  which we have verified through molecular dynamics simulations. A series of simulations were performed on nanotwinned specimens shown in Fig. 3 by replacing the fixed boundary conditions in the  $Y$ -direction with periodic boundary conditions in all directions. The specimens were first equilibrated at 800 K under the NPT ensemble to relax the stresses and then subjected to uniaxial tension. The Young's modulus was obtained in each case as the slope of the stress-strain curve. For each CTB spacing, an identical simulation was performed on a corresponding single crystalline specimen. Figure 6 shows that the values of  $E_{NT}$  and  $E_{SC}$  converge for CTB spacing larger than 1 nm. Although some size effect is observed for spacings less than 1 nm, the difference is only about 4%, so our assumption that  $E_{NT} \approx E_{SC}$  remains valid. We note that this analysis can be used to estimate the thermal stress due to any type of GB. Indeed, previous studies have demonstrated that the thermal expansion coefficient of a general GB follows a  $1/d$  dependence on the grain size or GB spacing [16,20]. Thus, our study concludes that the thermal stress should exhibit a  $1/d$

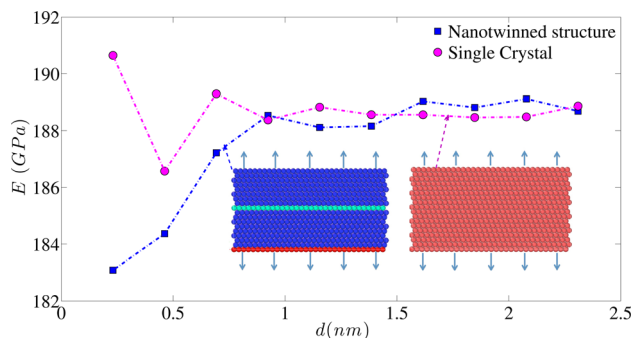


**Fig. 6 Variation of the Young's Modulus for single crystal ( $E_{SL}$ ) and nanotwinned ( $E_{NT}$ ) specimen with CTB spacing  $d$  at 800 K**

dependence for any interface and that it arises from the inhomogeneity in the coefficient of thermal expansion caused by the interfacial region around the CTB or GB.

## 5 Numerical Estimates

Based on the simulation results and the theoretical model discussed above, we now estimate the coefficient of thermal expansion for a CTB and compare it with available estimates for GBs. To this end, let  $m$  be the slope of the linear fit for  $\sigma$  versus  $1/d$ . Then, using the expression for the slope based on Eq. (4), we have

$$\Lambda(\alpha_{TB} - \alpha_{SC}) = \frac{m}{E_{SC} \Delta T} \quad (5)$$

Since  $\Lambda$  is not known, we estimate the value of the product of the  $\Lambda$  parameter and the difference in the thermal expansion coefficients of the CTB and the single crystal. Normalizing the above expression with  $\alpha_{SC}$  and the lattice constant,  $a$ , we define  $\kappa$  as

$$\kappa = \frac{\Lambda}{a} \left( \frac{\alpha_{TB}}{\alpha_{SC}} - 1 \right) = \frac{m}{a \Delta T E_{SC} \alpha_{SC}} \quad (6)$$

We use the following numerical values for Cu:  $a = 3.615 \text{ \AA}$  (at 0 K),  $E_{SC} = 189 \text{ GPa}$  (Fig. 6), and  $\alpha_{SC} = 16.934 \times 10^{-6} / \text{K}$  (obtained from simulations). Thus, calculating the slope,  $m$ , from Fig. 2 and substituting in Eq. (6), we get

$$\kappa = \frac{\Lambda}{a} \left( \frac{\alpha_{TB}}{\alpha_{SC}} - 1 \right) = 0.1772 \quad (7)$$

Similarly, calculating the slopes for the curves for different  $N$  from Fig. 4 and substituting in Eq. (6), we get  $\kappa = 0.1112$  for  $N = 3$ ,  $\kappa = 0.1386$  for  $N = 7$ , and  $\kappa = 0.1502$  for  $N = 11$ . Note that the values for  $\kappa$  approach that specified in Eq. (7) as  $N$  increases. To investigate this size effect in specimens with fewer atomic layers, let us consider a finite nanotwinned structure with  $N$  CTBs in the interior similar to our simulation specimens which are nonperiodic in the  $Y$ -direction. Since the structure is finite (non-periodic), it does not contain the interfacial regions of thickness  $\Lambda/2$  on the ends of the specimen, unlike the structure in Fig. 5 which is periodic. Then, Eq. (2) is modified to

$$d(N+1)\alpha_{NT} = N\Lambda\alpha_{TB} + (N+1)(d-\Lambda)\alpha_{SC} \quad (8)$$

which can be written as

$$\alpha_{NT} - \alpha_{SC} = \frac{\Lambda}{d} (\alpha_{TB} - \alpha_{SC}) - \frac{\Lambda\alpha_{TB}}{d(N+1)} \quad (9)$$

Thus, for very large  $N$ , Eq. (9) reduces to Eq. (2). Revisiting the results of Fig. 4, we see that for fixed  $d$ , as  $N$  increases, the second term on the right hand side reduces and the curves eventually converge to that of Fig. 2. Thus, the difference in the slopes in Fig. 4 arises due to finite size effects in specimen with very few CTBs.

We finally calculate the thermal expansion coefficient for the CTB based on estimates for  $\Lambda$  for different interfaces available in literature. A previous study estimated the thickness of the interfacial region for a general GB in nanocrystalline Cu and Au specimens to be about  $2a-3a$  [16]. Their atomistic simulations revealed that the thermal expansion coefficient of a twist GB in Au is about 80% greater than that of a single crystal for the smallest GB spacing considered. Experimental studies by Lu and Sui [20] reported the interfacial thickness of GBs in Ni-P alloys to be about 2 nm. Since CTB is a coherent, highly ordered interface, it is reasonable to assume that the interfacial thickness for a CTB would be much less than that of a GB. Indeed, in our recent work [21] using molecular dynamics simulations of the thermal fluctuations of

CTBs, we show that the average thickness of a CTB is about 0.1–0.2 Å. Using  $\Lambda = 0.1$  Å in Eq. (7), we obtain  $\alpha_{\text{TB}} = 7.4\alpha_{\text{SC}}$

This is consistent with the range for the thermal expansion coefficient of GBs reported by Lu and Sui [20] between 1.2 and 12 times that of a single crystal.

## 6 Concluding Remarks

In summary, we present molecular dynamics simulations to estimate the thermal stress due to the presence of parallel CTBs at finite temperature. Our simulations reveal that for all twin boundary spacings,  $d$ , the stress decays as  $1/d$ . We present a simple analytical model to show that the  $1/d$  dependence stems from the thermal stress in nanostructured materials due to the inhomogeneity in the thermal expansion coefficient of the matrix and the interfacial regions. It is also interesting to note that twin boundaries separated by a mere distance of about 6 Å lead to a thermal expansion induced stress of about 250 MPa which is surprisingly large. This possibly results from the large coefficient of thermal expansion of a CTB which is more than seven times greater than that of a single crystal. However, we note that these results are obtained for nanotwinned specimens when the thermal stress is not relaxed. If the thermal stress is relaxed completely, there will be no stress measured from simulations. The environment experienced by twin boundaries in real nanotwinned materials should be somewhere in between the two cases. This is because of residual thermal stress within the grains in a typical nanocrystalline structure resulting from the different thermal expansion of neighboring grains and the GB regions separating them [16]. Thus, the present work provides an upper bound to the thermal expansion induced stress in the presence of twin boundaries and other crystalline interfaces. We finally note that although our simulations and analysis should hold for GBs in general, our study focuses on twin boundaries owing to the fabrication of nanotwinned structures consisting of parallel twin boundaries with separation distances ranging from a few nanometers to a few angstroms.

## Acknowledgment

We gratefully acknowledge the support of NSF under Grant No. CMMI-1129041 and DARPA under Grant No. N66001-10-1-4033. The simulations were performed on the supercomputing facility hosted by the Research Computing Center at University of Houston.

## References

- [1] Lu, L., Shen, Y., Chen, X., Qian, L., and Lu, K., 2004, "Ultra-high Strength and High Electrical Conductivity in Copper," *Science*, **304**(5669), pp. 422–426.
- [2] Zhang, X., Wang, H., Chen, X. H., Lu, L., Lu, K., Hoagland, R. G., and Misra, A., 2006, "High-Strength Sputter-Deposited Cu Foils With Preferred Orientation of Nanoscale Growth Twins," *Appl. Phys. Lett.*, **88**(17), p. 173116.
- [3] Hodge, A. M., Wang, Y. M., and Barbee, Jr., T. W., 2008, "Mechanical Deformation of High-Purity Sputter-Deposited Nano-Twinned Copper," *Scr. Mater.*, **59**(2), pp. 163–166.
- [4] Lu, K., Lu, L., and Suresh, S., 2009, "Strengthening Materials by Engineering Coherent Internal Boundaries at the Nanoscale," *Science*, **324**(5925), pp. 349–352.
- [5] Kulkarni, Y., Asaro, R. J., and Farkas, D., 2009, "Are Nano-Twinned Structures in FCC Metals Optimal for Strength, Ductility, and Grain Stability," *Scr. Mater.*, **60**(7), pp. 532–535.
- [6] Kulkarni, Y., and Asaro, R. J., 2009, "Are Some Nano-Twinned FCC Metals Optimal for Strength and Grain Stability," *Acta Mater.*, **57**(16), pp. 4835–4844.
- [7] Dao, M., Lu, L., Shen, Y. F., and Suresh, S., 2006, "Strength, Strain-Rate Sensitivity and Ductility of Copper With Nanoscale Twins," *Acta Mater.*, **54**(20), pp. 5421–5432.
- [8] Bezares, J., Jiao, S., Liu, Y., Bufford, D., Lu, L., Zhang, X., Kulkarni, Y., and Asaro, R. J., 2012, "Indentation of Nano-Twinned FCC Metals: Implications for Nano-Twin Stability," *Acta Mater.*, **60**(11), pp. 4623–4635.
- [9] Demkowicz, M., Anderoglu, O., Zhang, X., and Misra, A., 2011, "The Influence of Sigma 3 Twin Boundaries on the Formation of Radiation-Induced Defect Clusters in Nanotwinned Cu," *J. Mater. Res.*, **26**(14), pp. 1666–1675.
- [10] Yu, K. Y., Bufford, D., Sun, C., Liu, Y., Wang, H., Kirk, M. A., Li, M., and Zhang, X., 2013, "Removal of Stacking-Fault Tetrahedra by Twin Boundaries in Nanotwinned Metals," *Nat. Commun.*, **4**(1377), pp. 1–7.
- [11] Jang, D., Li, X., Gao, H., and Greer, J. R., 2012, "Deformation Mechanisms in Nanotwinned Metal Nanopillars," *Nat. Nanotechnol.*, **7**(9), pp. 594–601.
- [12] Wang, J., Sansoz, F., Huang, J., Liu, Y., Sun, S., Zhang, Z., and Mao, S. X., 2013, "Near-Ideal Theoretical Strength in Gold Nanowires Containing Angstrom Scale Twins," *Nat. Commun.*, **4**(1742), pp. 1–8.
- [13] Hammami, F., and Kulkarni, Y., 2014, "Size Effects in Twinned Nanopillars," *J. Appl. Phys.*, **116**(3), p. 033512.
- [14] Mishin, Y., Mehl, M. J., Papaconstantopoulos, D. A., Voter, A. F., and Kress, J. D., 2001, "Structural Stability and Lattice Defects in Copper: Ab Initio, Tight-Binding, and Embedded-Atom Calculations," *Phys. Rev. B*, **63**(22), p. 224106.
- [15] Plimpton, S. J., 1995, "Fast Parallel Algorithms for Short-Range Molecular Dynamics," *J. Comp. Phys.*, **117**(1), pp. 1–19.
- [16] Phillpot, S. R., 1992, "Thermoelastic Behavior of Grain-Boundary Superlattices," *J. Appl. Phys.*, **72**(12), pp. 5606–5615.
- [17] Klam, H. J., Hahn, H., and Gleiter, H., 1987, "The Thermal Expansion of Grain Boundaries," *Acta Metall.*, **35**(8), pp. 2101–2104.
- [18] Wagner, M., 1991, "Structure and Thermodynamic Properties of Nanocrystalline Metals," *Phys. Rev. B*, **45**(2), pp. 635–639.
- [19] Jaszczak, J. A., and Wolf, D., 1992, "Thermoelastic Behavior of Structurally Disordered Interface Materials: Homogeneous Versus Inhomogeneous Effects," *Phys. Rev. B*, **46**(4), pp. 2473–2480.
- [20] Lu, K., and Sui, M. L., 1995, "Thermal Expansion Behavior in Nanocrystalline Materials With a Wide Grain Size Range," *Acta Metall. Mater.*, **43**(9), pp. 3325–3332.
- [21] Chen, D., and Kulkarni, Y., "Entropic Interactions Between Fluctuating Twin Boundaries," (to be submitted).